IN-VENTO 2026
International Conference of the Italian Association for Wind Engineering
Bari, September 13th – 16th, 2026

VIV–Galloping of tandem circular cylinders in sub-critical and post-critical regimes

Verel Chanya Djomo[a], Edouard Verstraelen[a], Thomas Andrianne[a]

[a]*Aeroelasticity and Experimental Aerodynamics, University of Liège, Belgium*

SUMMARY:
The aim of this work is to develop mathematical models describing the interaction between VIV and galloping of tandem circular cylinders, in sub-critical and post-critical regimes. This model requires experimental data as empirical input and validation purposes. Experiments around flexible cylinders are conducted in air to investigate sub-critical regimes while post-critical data are taken from Dubois, 2024. Several tandem configurations are studied, including perfect alignment ($T/D = 0$), staggered arrangements ($T/D \neq 0$), with the upstream cylinder fixed, or flexible. Pressure sensors will be used in static and dynamic tests to obtain pressure coefficients and forces acting on each cylinder, in order to calibrate the model. The equations of motion of the aeroelastic system are therefore formulated as generic differential equations with parameters to identify.

Keywords: galloping, viv, tandem cylinders, wind tunnel, flow regimes, wake interactions

1. INTRODUCTION

Modeling the interaction between VIV and galloping remains challenging in many wind engineering applications. Most studies concentrate on square or rectangular cross-sections (Mannini et al., 2017; Han et al., 2021). For a single circular cylinder, an additional instability source is required. For example, Nakamura et al., 1994 used a long splitter plate to trigger this interaction around a single circular cylinder. In the present work, a second circular cylinder, flexible or rigid is added upstream from the flexible cylinder to produce wake interactions. The aeroelastic responses of the cylinders are strongly influenced by the flow regime. The purpose of this work is to model interactions between VIV and galloping in sub- and post- critical regimes ($1.5 \cdot 10^2 \leq Re \leq 3 \cdot 10^5$ and $Re \geq 3.5 \cdot 10^6$ respectively (Lienhard, 1966)), relying on measured forces and pressure characteristics acting on each cylinder (static and dynamic).

2. EXPERIMENTAL DATA

Experimental tests are conducted in the low-subsonic wind tunnel laboratory of University of Liège. For tandem configurations in sub-critical regimes, the two cylinders are smooth and have a diameter of $D = 125$ mm and a height of $H = 600$ mm, with the upstream cylinder being rigid. They are separated by $L/D = 3$ in the streamwise direction, to reproduce the same flow regimes of an isolated cylinder around the front cylinder. According to Dubois and Andrianne, 2022, up to $L/D = 1.8$, the variations of the time-averaged drag and lift coefficients of the upstream cylinder are close to those of a single cylinder. Increasing the spacing to $L/D = 3$ is therefore expected to further reproduce the same pattern, while enhancing a proximity-and-wake-interference (P+W) on the downstream cylinder (Zdravkovic, 1988). Figure 1a shows a schematic of the configurations, by highlighting the streamwise and crossflow spacings L and T, respectively. The Scruton number, defined as $S_c = \frac{4\pi\, m_s \zeta_s}{\rho\, D^2}$, is equal to 0.84, with ζ_s the structural damping ratio, ρ the air density and m_s the structural mass of the translating system. Three crossflow configurations are considered : the cylinders are either aligned ($T/D = 0$), or the front cylinder is shifted by $T/D = 0.34$ or $T/D = 0.68$. For each of these configurations, the streamwise spacing is always $L/D = 3$. Figure 1b illustrates a rear view of the setup with $T/D = 0.34$.

Post-critical experiments were conducted by Dubois, 2024. They involve two rough cylinders ($D = 125$ mm, $H = 1250$ mm) both free to move and were performed in the same wind tunnel. The cases chosen for modeling correspond to the purely tandem arrangement ($T/D = 0$) with $L/D = 1.2$ and $L/D = 1.8$. For each spacing, two Scruton numbers are considered: $S_c = 3.9$ & 14.1.

The table of Figure 1 summarizes the main characteristics of the two experimental setups considered in this work.

(a) Schematic of the generic setup **(b)** Backview setup with $T/D = 0.34$ **(c)** Setup of Dubois, 2024

Cases	Sub-critical regimes	Post-critical regimes	Post-critical regimes
L/D	3	1.2	1.8
T/D	0.34 & 0.68	0	0
S_c [-]	0.84	3.9 & 14.1	3.9 & 13.5

Figure 1. Experimental setups

Figure 2 describes aeroelastic responses of the cylinders in sub- and post-critical regimes. The following observations will highlight additional physical effects that must be considered when modeling VIV and galloping interactions.

In subcritical regimes, three relevant comments are noticeable. (i) In tandem and staggered configurations, the onset of vibrations is observed at significantly lower reduced velocity U_r ($U_r = \frac{U_\infty}{f_n D}$ where U_∞, f_n, D are respectively the wind speed, natural frequency and diameter of cylinders) compared to the response of the isolated cylinder : vibrations starts around $U_r = 3.25$ which is well below the critical VIV velocity of the single cylinder, here associated with $1/St = 4.8$. This is because the downstream cylinder is not excited by its own vortex shedding but by the unsteady wake generated upstream (Assi, 2014). (ii) In perfect alignment ($T/D = 0$), only VIV occurs as the rear cylinder remains in the (a)-symmetric wake of the upstream one. (iii) For staggered configurations, VIV is followed by another increase in amplitude until the same level of the maximum amplitude of vibrations of the single cylinder. Here, the offset introduces an initial asymmetry in the wake interaction, characterized by a gap-flow switching mechanism (Zdravkovic, 1988). This mechanism tends to realign the downstream cylinder behind the upstream one, thereby generating a transverse force that sustains the oscillations and drives the transition from a wake-induced response to a VIV–galloping regime. Depending on the initial gap, this force may either decay or persist (after $U_r = 6.5$). All these three observations justify the inclusion of dynamic coupling terms accounting for both the wake of the upstream cylinder and the motion of the downstream cylinder, as proposed in Section 3.

Concerning post-critical regimes, the aeroelastic responses depend on the spacing (L/D): it corresponds to VIV–galloping interactions for $L/D = 1.2$ or pure VIV with possible VIV–galloping interactions for $L/D = 1.8$, as identified by Dubois, 2024.

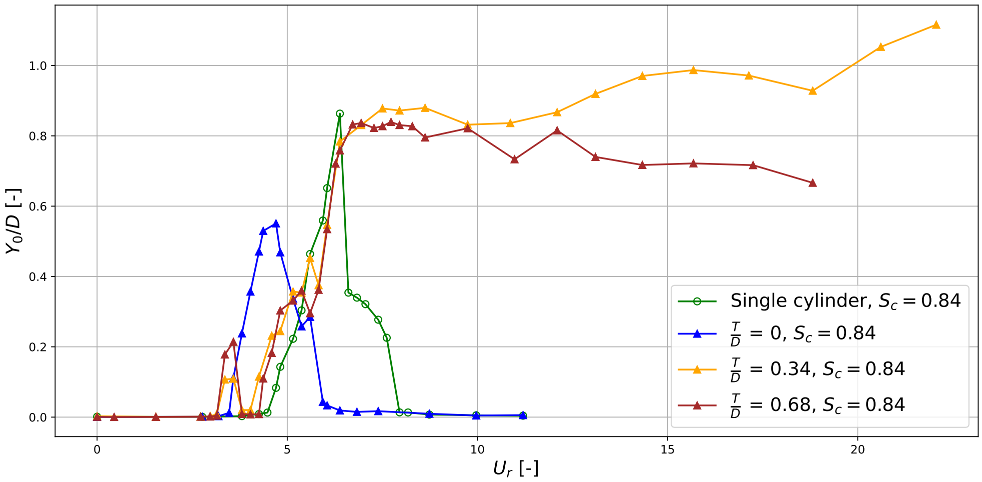

(a) Sub-critical regime, $\frac{L}{D} = 3$

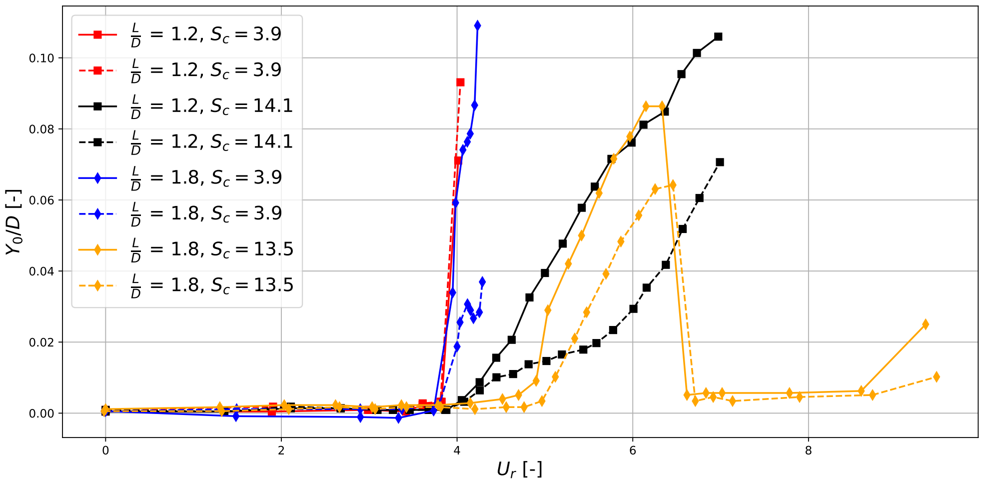

(b) Post-Critical regime, $\frac{T}{D} = 0$

Figure 2. Aeroelastic responses in both regimes: solid lines represent the rear cylinder, while dashed lines represent the upstream cylinder.

3. MODELING

The dynamics of the system – regardless the regime – are characterized by two main degrees of freedom for each cylinder : $Y_i = y_i/D_i$ and α_i, representing respectively the dimensionless crossflow displacement of the cylinder and the angular displacement of the wake, as proposed by Tamura and Matsui, 1979. Therefore, the model consists of a system of four main differential equations. These equations can be reduced to three, depending on whether the upstream cylinder is fixed ($Y_u = 0$) or whether the spacing L/D results in a single wake for both cylinders. The first case corresponds to the present sub-critical regimes, whereas the second reflects the experimental configurations investigated in Dubois, 2024.

Subscripts $._u$ and $._d$ denote the upstream and downstream cylinder, respectively. In a general form, it can be written that : $\alpha_u = f(Y_u, Y_d, \alpha_d)$, $\alpha_d = f(Y_d, Y_u, \alpha_u)$, $Y_d = f(Y_u, \alpha_u, \alpha_d)$ and $Y_u = f(Y_d, \alpha_u, \alpha_d)$. This simply means that each variable are coupled to the others. Based on the model of Tamura and Matsui, 1979 and taking into account existing model development like Mannini et al., 2017 and Dubois and Andrianne, 2023, here below are the four generic equations :

$$\ddot{Y}_u + [2\eta + n(f + C_D)\frac{\nu}{S^\star}]\dot{Y}_u + Y_u = -fn\nu^2\frac{\alpha_u + \alpha_d}{S^{\star 2}} + A_w(U_r, \dot{Y}_u, \dot{Y}_d, Y_u, Y_d, L/D, T/D) \tag{1}$$

$$\ddot{Y}_d + [2\eta + n(f + C_D)\frac{\nu}{S^\star}]\dot{Y}_d + Y_d = -fn\nu^2\frac{\alpha_u + \alpha_d}{S^{\star 2}} + B_w(U_r, \dot{Y}_u, \dot{Y}_d, Y_u, Y_d, L/D, T/D) \tag{2}$$

$$\ddot{\alpha}_u - 2\zeta\nu[1 - (\frac{4f^2}{C_{L0}^2})\alpha_u^2]\dot{\alpha}_u + \nu^2\alpha_u = C_w(U_r, \ddot{Y}_u, \ddot{Y}_d, \dot{Y}_u, \dot{Y}_d, L/D, T/D) \tag{3}$$

$$\ddot{\alpha}_d - 2\zeta\nu[1 - (\frac{4f^2}{C_{L0}^2})\alpha_d^2]\dot{\alpha}_d + \nu^2\alpha_d = D_w(U_r, \ddot{Y}_u, \ddot{Y}_d, \dot{Y}_u, \dot{Y}_d, L/D, T/D) \tag{4}$$

The notation of Tamura and Matsui, 1979 is used. In sub-critical regimes, Equation 1 disappears as well as any terms related to Y_u in the other equations. In post-critical regimes and in particular with $1.2 \leq L/D \leq 1.8$, Equations 3 & 4 merge into one equation since a single wake is formed (Zdravkovic, 1988, Dubois and Andrianne, 2023). Terms A_w, B_w, C_w and D_w have to be identified to make explicit the full system of differential equations. Dubois and Andrianne, 2023 proposed A_w and B_w as the quasi-steady aerodynamic force coefficients acting on each cylinder. These coefficients can be extracted from experiments on static or dynamic measurements. In addition, terms C_w and D_w describe the effect of cylinders' motions on the wake dynamics. They will be identified from unsteady pressure field measured on oscillating cylinders. Globally, the parameters of these additional terms govern their contribution to the systems.

REFERENCES

Assi, G. R. S. (2014). Wake-induced vibrations of tandem and staggered cylinders with two degree of reedom. Journal of Fluids and Strutures 50, 340–357.

Dubois, R. (2024). Flow-induced vibrations of twin cylinders in the post-critical regime. Ph.D. Dissertation, University of Liège, Liège, Belgium.

Dubois, R. and T. Andrianne (2022). Flow around tandem rough cylinders: Effects of spacing and flow regimes. Journal of Fluids and Strutures 109, 103465.

Dubois, R and T. Andrianne (2023). Modelling flow-induced vibrations of tandem cylinders in the post-critical flow regime. Proceedings of 16th International Conference on Wind Engineering. [Paper presentation]. Florence, Italy.

Han, P., P. Hémon, E. de Langre, and G. Pan (2021). Nonlinear modeling of combined galloping and vortex-induced vibration of square sections under flow. Nonlinear Dynamics 103, 3113–3125.

Lienhard, J. H. (1966). *Synopsis of Lift, Drag, and Vortex Frequency Data for Rigid Circular Cylinders*. Tech. rep. Washington State University, Pullman, Washington.

Mannini, C., T. Massai, A. M. Marra, and G. Bartoli (2017). Interference of vortex-induced vibration and galloping: experiments and mathematical modelling. Procedia Engineering 199, 3133–3138.

Nakamura, Y., K. Hirata, and K. Kashi (1994). Galloping of a circular cylinder in the presence of a splitter plate. Journal of Fluids and Strutures 8, 355–365.

Tamura, Y. and G. Matsui (1979). Wake-oscillator model of votex-induced oscillation of ciruclar cylinder. Pergamon 2, 1085–1092.

Zdravkovic, M. M. (1988). Review of interference-induced oscillations in flow past two parallel circular cylinders in various arrangements. Journal of Wind Engineering and Industrial Aerodynamics 28, 183–200.